Electromagnetic resonances of a single grating of cylinders in the dipole approximation

May-August 1999

Sir Frank Packer Theoretical Physics Department School of Physics
University of Sydney

Stage de deuxième année du magistère

Directeur de stage : Pr. Ross C. McPhedran
Directeur du laboratoire : Pr. Don Melrose
Boris Kuhlmey, Département des Sciences de la Matière, ENS Lyon, France

Abstract

With the aim of explaining anomalous peaks in the optical absorption spectrum of stacked gratings of cylinders, which are photonic bang gap material, we study the resonances of a single grating theoretically. We derive the main equation of the resonances using the Generalized Rayleigh Method and truncate it to the second order of multipole expansion. We investigate extensively the behaviour of the roots of this equation numerically and analytically in the case of normal incidence. The work on the more general case of off-axis incidence is not finished yet but preliminary results are given. Achieving the analysis of the off-axis case is essential if we want to obtain insights in the behaviour of stacked gratings.

Introduction

In recent years a lot of work has been done on the theory and applications of 'photonic crystals' or photonic band gap materials [1].

The prospect of having materials with similar properties for photons as semiconductors have for electrons stirred up the academic scientific community as well as the industry: applications would range from high efficiency fibre optics to highly integrated optics likely to make completely optical computers a reality.

On the more fundamental level, constructing crystals for light instead of for electrons, studying the properties of those new materials and drawing parallels between solid state physics and optics of diffracting materials are also highly interesting.

Photonic band gap materials are periodically arranged conductors or dielectrics, in one, two or three dimensions. Using Bloch-Floquet's theorem with the periodicity of the boundary conditions imposed by such a material on the electromagnetic field leads to general properties very similar to those the same theorem gives in solid state physics for electrons in a crystal.

There are two approaches for the theoretical analysis of the detailed properties of photonic band gap materials. The first work was made mostly by solid state scientists and is therefore very similar to theoretical work on crystals: the electromagnetic fields are evaluated numerically with techniques based on finite differences or plane wave expansions[2]. More recently, advances in diffraction theory have made possible a new approach, based on the Generalized Rayleigh Method and on the computation of lattice sums. The techniques emerging of this approach have proven to be very accurate and to use modest computer resources compared to other techniques.

The Theoretical Physics Department of the University of Sydney is one of the leading teams in this new field, and offered me the chance to help them in their research on surface and defect states of photonic band gap materials: As for electrons, a photonic band gap means that photons of certain energy levels and directions can not propagate through the material[1]. If there is a defect in the material, or an interface to another material (which can also be seen as a defect) it is in some cases possible to limit the propagation of light to those defects. Very unusual propagation characteristics of light can then be achieved, examples of which are microscopic resonant cavities,

[1]But in contrast to electrons, a third dependence is very significant for photons: the polarization dependence.

lossless waveguide bends or perfect channel drop filters [3]. The study of what exactly happens around the defects including the role of defect states is therefore of high importance.

In the case of a two dimensional photonic crystal, one can see the arrangement of dielectrics or conductors as a stack of gratings [4]. Studying a finite or semi-infinite number of stacked gratings let the surface phenomena appear on the interface with the region without gratings. The properties of stacked gratings can be found through iterative multiplications of scattering matrices, but in order to explain the results physically, one has to be aware of all the properties of a single grating.

My task was therefore to study the resonances of a single grating, with the hope of finding possible clues for the interpretation of unexplained peaks in stacked-gratings band gaps. Indeed resonance effects had shown to be of great importance in similar problems [5][6][7].

In the first part we will introduce the geometry of the problem and discuss the Rayleigh method which yields the main equation we will use to find the resonances. In the second part, we will concentrate on resonances in the case of normal incidence: our main equation is greatly simplified in that case, so that we can distinguish three kind of roots according to their symmetry. The behaviour of one kind of these roots with varying wavelength will be studied first numerically and then analytically. The much more complex case of off-axis incidence will be introduced in the third part.

1 Equation of the resonances

1.1 Geometry of the problem

We consider a single grating of cylinders of radii a and complex refractive index $n = n_r + in_i$[2], in the (Oxz) plane, periodically spaced by the distance d, under incidence of polarized light (see figure 1). The axis of the cylinders are parallel to the z-axis. Let $\mathbf{k_0}$ be the wave vector of the incident light and λ its wavelength. We have $k_0 = 2\pi/\lambda$. We will only consider the *classical* incidence (as opposed to the *conical* incidence), where $\mathbf{k_0}$ remains in the

[2]Due to the space-time linearity of Maxwell's equations, only the ratio of the index outside and inside of the cylinders is important for the physics of this problem. We will therefore use an outside refractive index of 1, as if the cylinders were in vacuum. If they are not, the refractive indices we will compute are the ratios to the outside refractive index. A similar argument will lead us to take $d = 1$, see footnote 8

Oxy plane. An unique angle is therefore sufficient to describe the direction of $\mathbf{k_0}$: We will call θ_0 the angle of incidence with respect to the Oy-axis.

We will consider the two main polarizations $\mathbf{E}_{||}$ and $\mathbf{H}_{||}$, in which the electric and magnetic fields are respectively aligned with the axis of the cylinders. In these cases, we will denote by V the component E_z or H_z of the field parallel to the cylinders, which satisfies the Helmholtz equation

$$(\nabla^2 + k_0^2)V(\mathbf{r}) = 0.$$

The spatial part of the incoming light can be written as[3]

$$V_{incident}(\mathbf{r}) = V_0 e^{i(k_0 x \sin\theta_0 - k_0 y \cos\theta_0)}.$$

In section 2 we will consider the analytically more simple case of normal incidence ($\theta_0 = 0$), the general case of off-axis (but non conical) incidence will be introduced in section 3.

1.2 The Generalized Rayleigh Identity (GRI)

Near and in the cylinders the field can be written as a multipole expansion (Bessel function expansion) in cylindrical coordinates. For the cylinder centred on the origin, one has outside the cylinder

$$V(r,\theta) = \sum_{m\in\mathbb{Z}} \left(A_m J_m(k_0 r) + B_m Y_m(k_0 r)\right) e^{im\theta} \ ,$$

[3]In most papers V_0 is taken to be $k_0^{(-1/2)} \cos\theta_0$ in order to normalize the incident energy flux to unity.

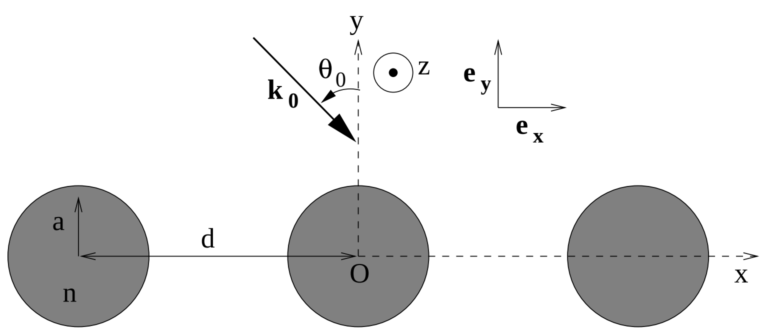

Figure 1: The geometry of the considered gratings

where J_m and Y_m are the usual Bessel and Neumann functions, r is the distance from the origin and θ is measured from the x-axis. This expression contains a regular part

$$\sum_{m\in\mathbb{Z}} \left(A_m J_m(k_0 r)\right) e^{im\theta}$$

and an irregular part which is not defined at the origin

$$\sum_{m\in\mathbb{Z}} \left(B_m Y_m(k_0 r)\right) e^{im\theta} \ .$$

Lord Rayleigh [8] was the first who put forward the hypothesis that the irregular part must be the contribution of the sources in the central cylinder, whereas the regular part must be the contribution from all other sources (other cylinders and sources at infinity, the last one being in our case the incident electromagnetic wave)[4].

Mathematically this yields

$$\sum_{m\in\mathbb{Z}} A_m J_m(k_0 r) e^{im\theta} = \sum_{m\in\mathbb{Z}} \sum_{p\in\mathbb{Z}^*} B_m Y_m(k_0|\mathbf{r}-\mathbf{R_p}|)) e^{im\arg(\mathbf{r}-\mathbf{R_p})} + V_0 e^{i(k_0 x\sin\theta_0 - k_0 y\cos\theta_0)} \tag{1}$$

where $\mathbf{R_p}$ is the position vector of the p-th cylinder with respect to the origin, *ie* $\mathbf{R_p} = pd\mathbf{e_x}$ and $\mathbf{r}$ is the position vector associated with (r,θ). By using addition theorems for Bessel functions (Graf's theorem) and a Bessel expansion of the incident field and then through equating the coefficients of the resulting expansion, one can simplify (1) to a set of equations, also known as the Generalized Rayleigh Identity (GRI):[5]

$$B_\ell - iA_\ell + \sum_{m\in\mathbb{Z}} S_{\ell-m} B_m = -i(-1)^l e^{-i\ell\theta_0} V_0 \tag{2}$$

where S_ℓ are global lattice sums defined in the general case as

$$S_\ell = \sum_{p=1}^{\infty} H_\ell^{(1)}(pk_0 d) \left[e^{ipdk_0\sin\theta_0} + (-1)^\ell e^{-ipdk_0\sin\theta_0} \right]$$

[4] In the same paper, he actually proved this result for a square array of cylinders, in the electrostatic case, using the Green theorem inside the unit cell. For a single grating the result is a bit more complicated to derive [9] and has been of interest only recently [10], as evaluating the involved lattice sums requires modern computers and recently discovered forms of the sums with better convergence[11][12].

[5] This method to derive the result has been used for arrays of cylinders, but in the case of a grating a direct integration of Green's theorem simplifies the proof. It has been included here to illustrate the *physical* meaning of the Rayleigh method. The complete proof can be found in [10].

with $H_0^{(1)}$ denoting the zeroth-order Hankel function of the first kind.

As the boundary conditions on the cylinder yield $A_\ell = -M_\ell B_\ell$ (see appendix A), we can write (2) in algebraic terms:

$$(M - iS)\mathbf{B} = \mathbf{E} \tag{3}$$

where

$$\mathbf{E}_\ell = (-1)^{\ell+1} V_0 e^{-i\ell\theta_0},$$

$\mathbf{B}$ is the vector of the multipole expansion of V, M is the (diagonal) boundary condition matrix given by

$$M_{l,m} = \begin{cases} \delta_{l,m} \frac{nJ_l'(nk_0a)Y_l(k_0a) - J_l(nk_0a)Y_l'(k_0a)}{nJ_l'(nk_0a)J_l(k_0a) - J_l(nk_0a)J_l'(k_0a)} & \text{, for } \mathbf{E}_{||} \\ \\ \delta_{l,m} \frac{J_l'(nk_0a)Y_l(k_0a) - nJ_l(nk_0a)Y_l'(k_0a)}{J_l'(nk_0a)J_l(k_0a) - nJ_l(nk_0a)J_l'(k_0a)} & \text{, for } \mathbf{H}_{||} \end{cases} \quad (l,m) \in \mathbb{Z} \tag{4}$$

and S is a lattice sum matrix given by

$$S_{l,m} = S_{l-m} + \delta_{l,m}$$

1.3 Resonances

We define as a resonance of the grating the set of parameters $\{\mathbf{k_0}, n\}$ for which the reflection and transmittance matrices are of infinite norm, *ie* there is a reflected and transmitted field without incoming light. Mathematically we will have a resonance for non zero $\mathbf{B}$ vectors with $\mathbf{E} = 0$, *ie* for zero-vectors of equation (3). As resonances imply non zero emitted energy (outgoing light) with no incoming energy, they can not be physically achieved without a source of energy inside the cylinders. We expect these resonances to appear for amplifying optical indices ($n_r > 0$ and $n_i < 0$) in the case of harmonic plane waves, or possibly with real indices in the case of a superposition containing only evanescent outgoing waves (complex $\mathbf{k_0}$).

1.4 Dipole approximation

For small radii (and in fact up to the order of $a/d = 0.3$) the dipole approximation is sufficient to describe the grating problem with good accuracy[6].

[6] Accuracy of the order of .01% for computing an equivalent conductivity of a square array of cylinders for example. See [13] for tables of the required order of the multipole expansion for a given accuracy, in the static case.

This approximation consists in truncating the $\mathbf{B}$ vector to three components ($\mathbf{B}_{-1}$ to $\mathbf{B}_1$) and thus truncating M and S to 3×3 matrices.

As we have $M_\ell = M_{-\ell}$ and $S_{-\ell} = (-1)^\ell S_\ell$, equation (3) becomes now

$$\begin{pmatrix} M_1 - iS_0 & -iS_1 & -iS_2 \\ iS_1 & M_0 - iS_0 & -iS_1 \\ -iS_2 & iS_1 & M_1 - iS_0 \end{pmatrix} \begin{pmatrix} B_{-1} \\ B_0 \\ B_1 \end{pmatrix} = \begin{pmatrix} 0 \\ 0 \\ 0 \end{pmatrix} \tag{5}$$

which can only have a solution if the associated determinant is zero:

$$(M_1 - i(S_0 + S_2)) \left[(M_0 - iS_0)(M_1 - i(S_0 - S_2)) - 2S_1^2 \right] = 0 \ . \tag{6}$$

Our work will now be to solve this equation and to analyse the behaviour of the roots when the different parameters vary.

2 Normal incidence

In the case off normal incidence[7], the lattice sums are greatly simplified so that our main equation (6) can be factorized into three simple terms. The roots of the simplified equations we obtain correspond to resonances of monopole and dipole symmetry, and their asymptotic behaviour can be investigated analytically.

2.1 The factorized equation

In the normal incidence case S_ℓ becomes

$$S_\ell = \sum_{p=1}^{\infty} H_\ell^{(1)}(pk_0 d) \left[1 + (-1)^\ell \right] . \tag{7}$$

The lattice sums of odd order now vanish, so that equation (6) becomes

$$(M_1 - i(S_0 + S_2))\,(M_1 - i(S_0 - S_2))\,(M_0 - iS_0) = 0 \ . \tag{8}$$

[7] One may wonder how the angle of incidence does influence a resonance as the resonance should happen with *no* incoming light. In fact $\mathbf{k}_0$ determines the pseudo-periodicity of the sources on the cylinders, in other words the relative phase of the sources. Exploring the resonances for different $\mathbf{k}_0$ is exploring different relative phases for the resonances. Physically a resonance will never be reached with non amplifying n, so what we are looking for is where the resonances come near to physically existing configurations, in which the angle of incidence and wavelength do have a significance.

Here the M's are a function of n, k_0, a and d, whereas the S's are a function of a, k_0 and d. As the computation of the S's is very slow, we will avoid to have to compute them in any root-finding subroutine. This can be easily done by choosing to solve (8) for n with given a, k_0, and d: the S's do not depend on n and need therefore to be computed only once before the root-finding loop is entered.

2.2 Monopole and dipole resonances

Solving (8) gives us two kinds of resonances. The structure of the field V associated with those roots does not depend upon numeric values of a and d, for each polarization the only dependence is on λ.

2.3 Monopole roots

The first root is $M_0 = iS_0$ and is associated with a monopole like eigenvector $\mathbf{B}_1 = \mathbf{B}_{-1} = 0, \mathbf{B}_0 = 1$: V is a linear combination of J_0 and Y_0, and has no angular dependence. A contour plot of the intensity of V for $\lambda = 4.6$ in $\mathbf{E}_{||}$ polarization is given in figure 2.

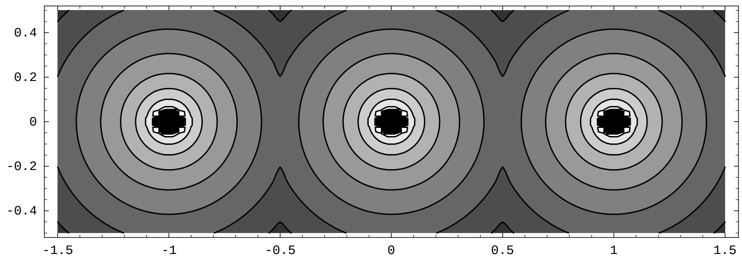

Figure 2: monopole resonance for $\lambda = 4.6d$

2.4 Dipole roots

The other roots are associated with eigenvectors with dipole symmetry:

$$\mathbf{B}_{\pm} = \begin{pmatrix} 1 \\ 0 \\ \pm 1 \end{pmatrix} \text{corresponding to the root } M_1 = i(S_0 \pm S_2)$$

Figure 3 shows the contour plot of V for $\mathbf{B}_+$ whereas figure 4 shows the contour plot of V for $\mathbf{B}_-$, both in $\mathbf{E}_{||}$ polarization. For $\mathbf{H}_{||}$ polarization the contour plots are slightly different, but their symmetries remain the same.

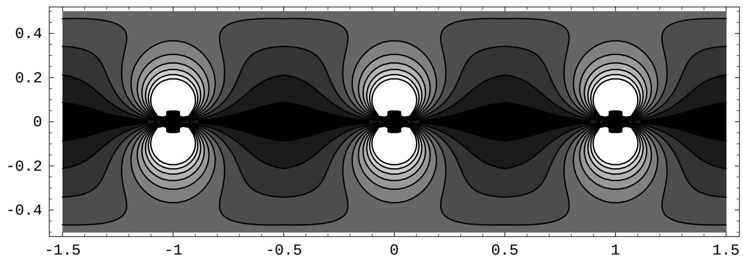

Figure 3: Contour plot of V for $\mathbf{B}_+$, $\lambda = 4.6d$

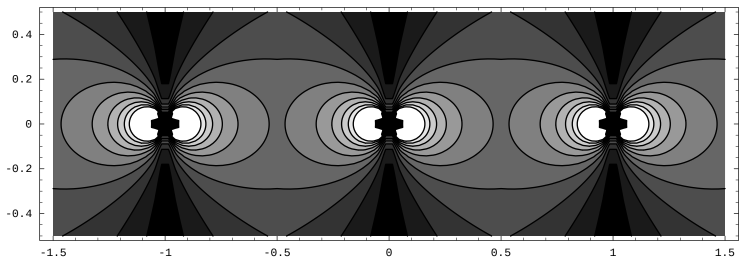

Figure 4: Contour plot of V for $\mathbf{B}_-$, $\lambda = 4.6d$

The symmetry of the field for the antisymmetric dipole resonances ($\mathbf{B}_-$) does not permit a coupling with the incoming light : It is antisymmetric along the Ox- axis whereas the incoming light (plane waves in normal incidence) is symmetric. We shall therefore not consider this root for further analysis. For the normal incidence case, we will concentrate on the monopole resonances. Nevertheless it is interesting to note that antisymmetric resonances would correspond to *real* optical indices ; we will see that in the off-axis case, where a coupling between those resonances and the light is possible, the indices become complex.

2.5 Numerical computation of monopole resonance roots

In order to solve $M_0 - iS_0 = 0$ where M and S are complex functions of a complex variable, we will write an equivalent equation which involves only analytic functions of n: (4) can be written

$$M_0(n,k_0,a) = \frac{N_0(n,k_0,a)}{D_0(n,k_0,a)}$$

where N_0 and D_0 are analytic functions of n, k_0 and a, so that

$$M_0 - iS_0 = 0 \Longleftrightarrow f_{k_0,a}(n) = N_0(n,k_0,a) - iS_0(k_0,a)D_0(n,k_0,a) = 0 \quad (9)$$

where $f_{k_0,a}(n)$ is an analytic function of n [8]. A Fortran program will then use the subroutine CROOT developed by Botten, Craig and McPhedran [14] to find the roots of this equation in the complex n-plane for a given a and λ in a circular region. Our program uses a combination of the methods developed by Twersky [11] and Nicorovici and McPhedran [12] to compute the otherwise very slowly convergent lattice sums S_ℓ.

For a given a we will investigate two aspects of the resonances : the evolution of a given root with the wavelength, and the asymptotic behaviour of the roots for large wavelengths.

The expression of M_0 being polarization dependent, we will begin with the $\mathbf{E}_{||}$ polarization and then consider the $\mathbf{H}_{||}$ polarization.

2.6 $\mathbf{E}_{||}$ polarization

In the $\mathbf{E}_{||}$ case $f_{k_0,a}(n)$ is even; figure 5 shows the set of roots in the complex n plane for an arbitrary $\lambda = 4.6$, given by a Mathematica root-finding program.

We shall now study the evolution of one of those roots with varying wavelength. A Fortran program will find the set of roots for the largest wavelength we are interested in (subsequently called the initial roots), and then track each root as λ decreases.

For a given a, the lattice sums depend only upon λ, they are therefore computed at the beginning of the program for every λ for which we want to find the roots.

Let $n_{\lambda_p,m}$ be the set of initial roots.

For each m, $n_{\lambda_{p-1},m}$, the root for λ_{p-1} is found by the CROOT subroutine in a disc centred on $n_{\lambda_p,m}$ and of arbitrary radius[9]. If more than

[8] Due to the scaling properties of the Maxwell equations, there is no change in the properties of the grating if all lengths are changed in the same proportions. Considering this, we will take $d = 1$ for all numerical computations, and express λ and a in 'units' of d

[9] The radius we used was determined by an analysis of the distance between two roots for several wavelengths, and is in fact dynamically adjusted to the current wavelength through an empirical formula.

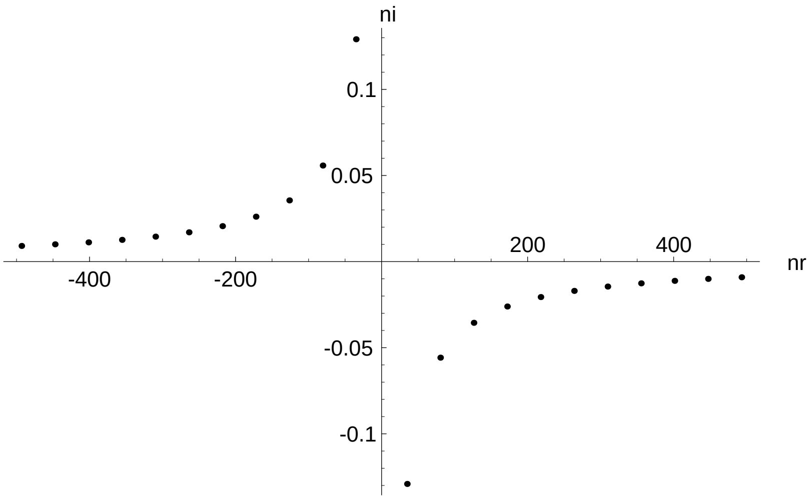

Figure 5: The set of n giving a resonance in $\mathbf{E}_{||}$ polarization for $\lambda = 4.6$

one root is found for λ_{p-1} in that disc, the program keeps the one which is nearest to $n_{\lambda_{p-1},m}$ [10]. If on the other hand no root is found, the algorithm continues the search in an annular region around the previous searching-disc until one root is found. For an example of the results, figure 6 (7) shows the evolution of the real (imaginary) part of the root closest to the origin versus λ.

2.6.1 Evolution of the roots with λ

Considering figures 6 and 7, we see that n tends to real positive values for sub-multiples of d. This is a general behaviour, independent of the actual value of a of the considered root, and is a well known natural resonance where the number of wavelengths occupying a grating period is an integer. Interesting optical behaviour occuring at such wavelength was first investigated by R.W. Wood [15].

For larger wavelengths we can observe two different behaviours: One root seems to scale like $\lambda^{1/2}$, whereas the other roots seem to scale like λ for their real part while their imaginary part tends to a constant (see figure 8-11). This behaviour will be explained in the next section.

[10]We are aware that in regions where trajectories of roots of different m are crossing, this arbitrary choice can lead to swapping of the m roots, and in the worst case we could even lose the track of one of the roots.

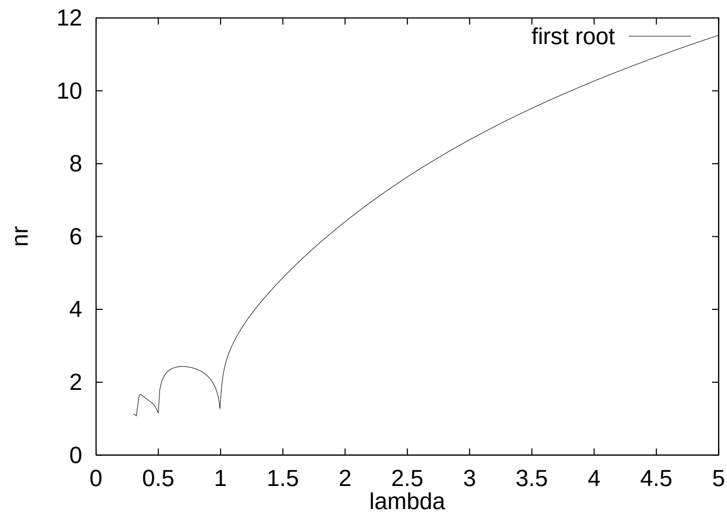

Figure 6: Real part of n for the root nearest to the origin in $\mathbf{E}_{||}$ polarization $\lambda/d \in [0.3, 5]$ ($a = 0.05d$, evaluation for 400 wavelengths in the considered interval)

2.6.2 Asymptotic behaviour

In this section we will consider the behaviour of the roots of (9) for large wavelengths and small radii. We will find simple formulas which approximate the whole set of resonances at a given large λ.

For $a \ll 1$ and $\lambda \gg 1$ we can approximate N_0, D_0 and S_0, if we bear in mind that as n seems to scale like λ at least in some of the cases, there is no reason for the product nk_0a to be necessarily infinitesimal.

One has:

$$J_0(k_0a) \approx 1 \qquad\qquad Y_0(k_0a) \approx \tfrac{2}{\pi} \ln k_0a$$

$$J_0(k_0a)' = -J_1(k_0a) \approx -\tfrac{k_0a}{2} \qquad Y_0(k_0a)' = -Y_1(k_0a) \approx \tfrac{2}{\pi k_0 a}$$

hence

$$N_0 \approx -\frac{2}{\pi}(nJ_1(nk_0a)\ln k_0a + \frac{1}{k_0a}J_0(nk_0a))$$

$$D_0 \approx -(nJ_1(nk_0a) + \frac{k_0a}{2}J_0(nk_0a))$$

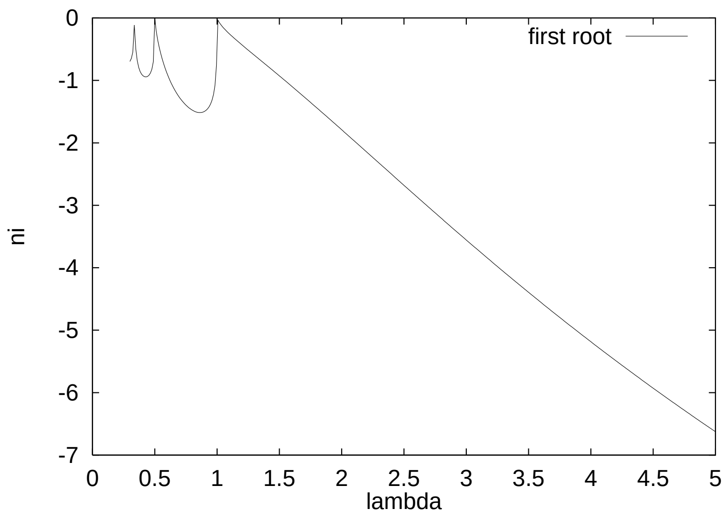

Figure 7: Imaginary part of n for the root nearest to the origin in $\mathbf{E}_{||}$ polarization $\lambda/d \in [0.3, 5]$ ($a = 0.05d$, evaluation for 400 wavelengths in the considered interval)

and following [11]

$$S_0 \approx \frac{2}{k_0 d} - i\frac{2}{\pi}\ln k_0 d$$

so that (9) becomes

$$\frac{nk_0 a J_1(nk_0 a)}{J_0(nk_0 a)} \approx \frac{1 + (k_0 a)^2 \ln k_0 d + i\frac{\pi k_0 a^2}{d}}{\ln a/d + i\frac{\pi}{k_0 d}} \tag{10}$$

We now simplify this equation by keeping only the main terms when k_0 approaches 0 and a remains constant (but small). (10) then becomes

$$\frac{nk_0 a J_1(nk_0 a)}{J_0(nk_0 a)} \approx \frac{1}{\frac{i\pi}{k_0 d}} = \frac{-ik_0 d}{\pi} \tag{11}$$

Here the right hand term tends to 0 as k_0 approaches 0.

First case: In this paragraph we will consider the case corresponding to the assumption that $nk_0 a$ remains bounded (consequently $J_1(nk_0 a)$ and $J_0(nk_0 a)$ remain bounded), and that $nk_0 a$ does not tend to zero. The only

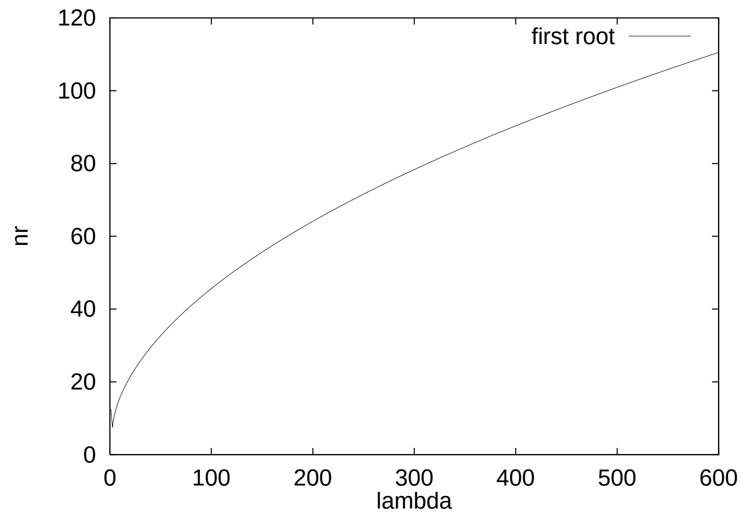

Figure 8: Real part of n for the root nearest to the origin in $\mathbf{E}_{||}$ polarization $\lambda/d \in [0, 600]$ ($a = 0.05d$, evaluation for 400 wavelengths in the considered interval)

way the left hand term can approach zero is that nk_0a tends to a root of J_1. A first approximation of the roots of (9) are therefore the roots of J_1 which can be approximated by

$$nk_0a \approx \pm\frac{(1+4m)\pi}{4},\ m \in \mathbb{N}$$

which gives us n:

$$n \approx \pm\frac{(1+4m)\lambda}{8a},\ m \in \mathbb{N} \tag{12}$$

This is a first order approximation for the resonant n, and gives us a good approximation of the real part of n. To get an approximation of the imaginary part, we will use a perturbation-like method:

We assume that the imaginary part n_i of n is a perturbation of n and use the result given by (12) (which we will call $n^{(0)}$) as a first order approximation of n. We use an approximation of $J_1(nk_0a)$ around $n^{(0)}$

$$J_1(nk_0a) \approx J_1(n^{(0)}k_0a)+J_1'(n^{(0)}k_0a)ik_0an_i = \frac{J_0(n^{(0)}k_0a) - J_2(n^{(0)}k_0a)}{2}ik_0an_i$$

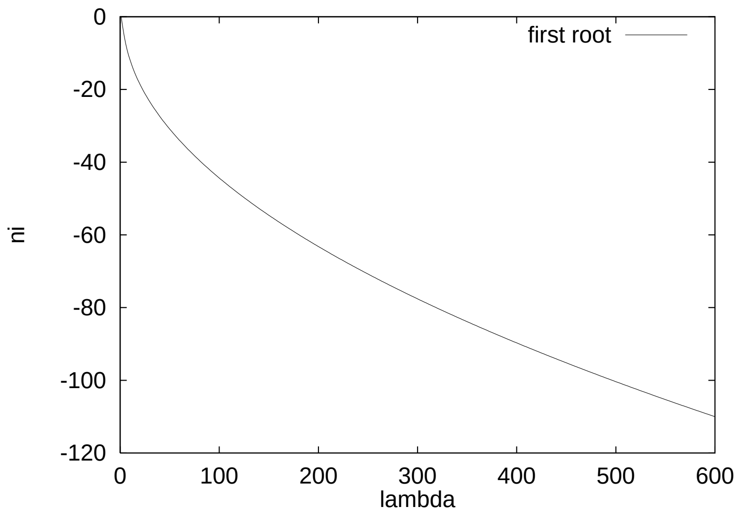

Figure 9: Imaginary part of n for the root nearest to the origin in $\mathbf{E}_{||}$ polarization $\lambda/d \in [0, 600]$ ($a = 0.05d$, evaluation for 400 wavelengths in the considered interval)

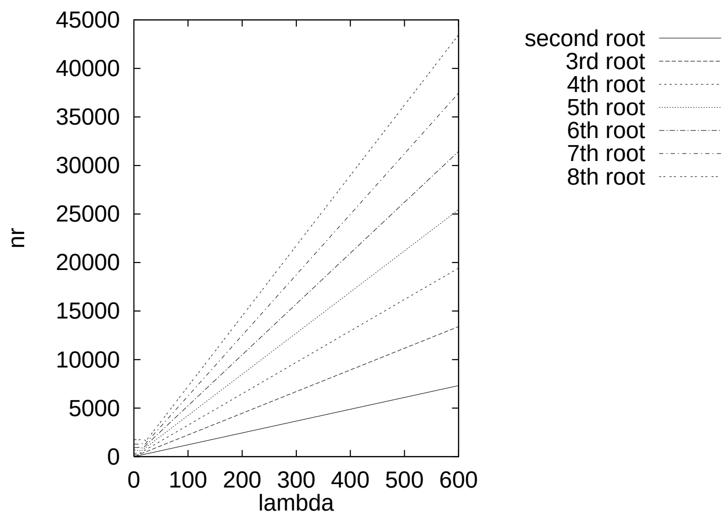

Figure 10: Real part of n for other roots in $\mathbf{E}_{||}$ polarization $\lambda/d \in [0, 600]$ ($a = 0.05d$, evaluation for 400 wavelengths in the considered interval)

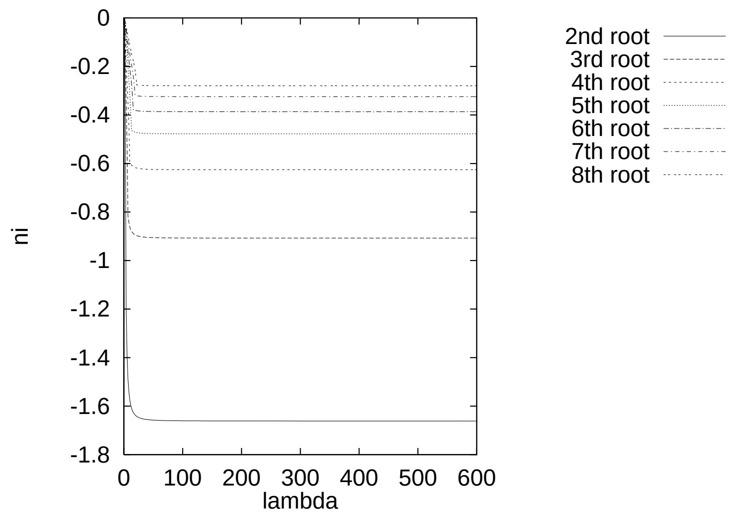

Figure 11: Imaginary part of n for other roots in $\mathbf{E}_{||}$ polarization $\lambda/d \in [0, 600]$ ($a = 0.05d$, evaluation for 400 wavelengths in the considered interval)

so that (11) becomes, to the first order in n_i,

$$\frac{n^{(0)}a^2(J_0(n^{(0)}k_0a) - J_2(n^{(0)}k_0a)}{2J_0(n^{(0)}k_0a)} in_ik_0 \approx -i\frac{d}{\pi} \; .$$

Using a recurrence formula of the Bessel functions, $J_1(n^{(0)}k_0a) = 0 = (J_0(n^{(0)}k_0a) + J_2(n^{(0)}k_0a))/2$, we can now easily extract an approximation of the imaginary part of n so that our complete approximation will be:

$$n_m(\lambda) \approx \mathrm{sign}(m)\left(\frac{(4|m|+1)\lambda}{8a} - i\frac{4d}{a\pi^2(1+4|m|)}\right), \; m \in \mathbb{Z} \tag{13}$$

Second case: We will now consider that nk_0a tends to zero when k_0 approaches zero. In this case we can simplify (11) using the first order approximation of $J_1(nk_0a)$ and $J_0(nk_0a)$:

$$\frac{nk_0a\frac{nk_0a}{2}}{1} \approx -i\frac{k_0d}{\pi}$$

and we have immediately

$$n \approx \pm(1-i)\sqrt{\frac{d\lambda}{2\pi^2a^2}} \tag{14}$$

Combining (13) and (14) we have found the complete set of roots: it is composed of two roots which scale like $\lambda^{1/2}$ and a discrete infinity of roots scaling like λ.

2.7 $\mathbf{H}_{||}$ polarization

In this case $f_{k_0,a}$ is odd: $n = 0$ is a trivial root of (9), but not of (8) and subsequently does not correspond to a physical solution. The methods used to find the resonances are very similar to the one used in 2.6. Changes will only appear in 2.7.2. For given λ and a, the set of resonances resembles figure 12.

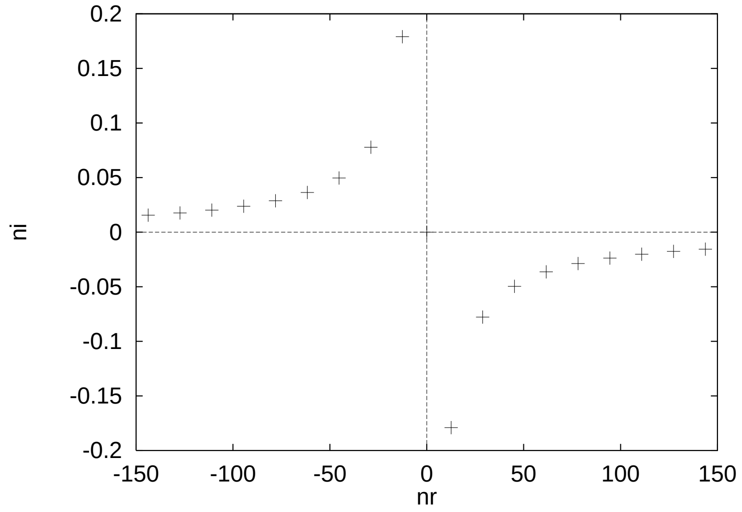

Figure 12: Set of resonating n for a grating with $a = 0.14d$ and $\lambda = 4.6$, $\mathbf{H}_{||}$ polarization

2.7.1 Evolution of the roots with λ

The typical evolution of a resonant n with λ for a given a is shown on figures 13 and 14. As for $\mathbf{E}_{||}$ polarization, we recognize the natural resonances of the grating for sub-multiples of d: the imaginary part of resonating n tends to zero for these values.

Unlike for $\mathbf{E}_{||}$ polarization, we now observe only one behaviour for all the roots for large wavelengths: As shown on figures 15 and 16 the real part of n

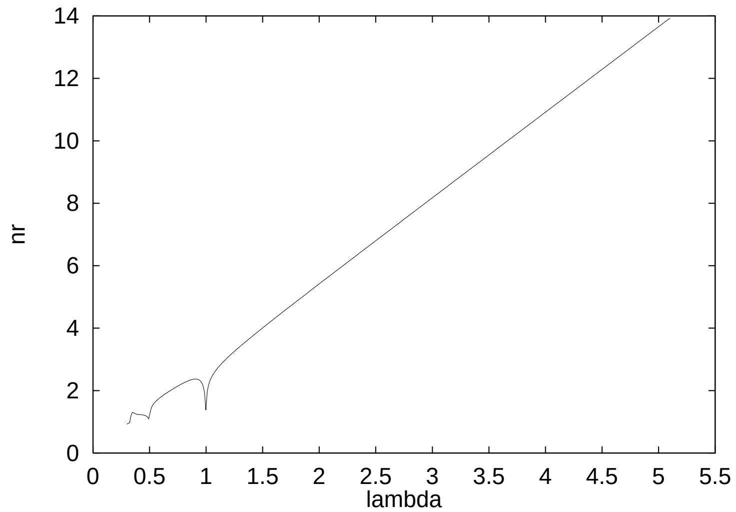

Figure 13: Grating resonances : Real part of one of the two symmetric roots nearest to the origin in $\mathbf{H}_{||}$ polarization. ($\lambda/d \in [0.3, 5]$, $a = 0.14d$, evaluation for 400 wavelengths in the considered interval)

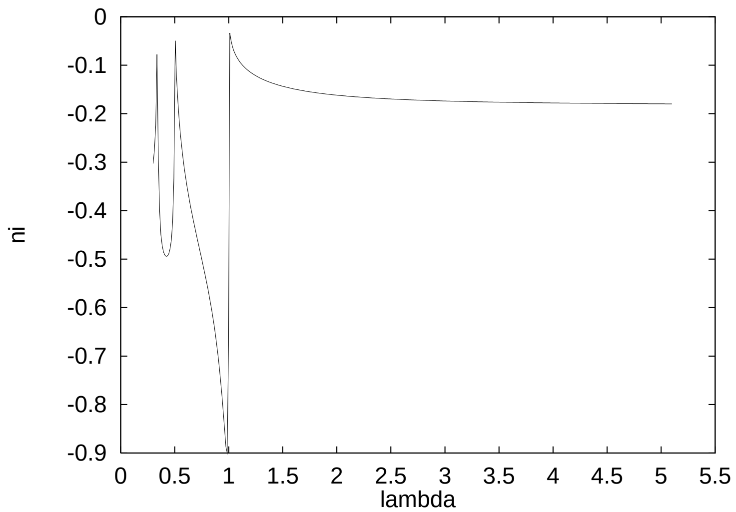

Figure 14: Grating resonances : Imaginary part of the same root as in fig. 13

seems to scale like λ for all roots, whereas the imaginary part of n tends to a constant. We will analyse this asymptotic behaviour in the next section.

2.7.2 Asymptotic behaviour

As in 2.6.2 we will consider the behaviour of the roots of (9) for large wavelengths and small radii. Using the same approximations we now find:

$$N_0 \approx -\frac{2}{\pi}\left(J_1(nk_0a)\ln k_0a + \frac{n}{k_0a}J_0(nk_0a)\right)$$

and

$$D_0 \approx -\left(J_1(nk_0a) + \frac{nk_0a}{2}J_0(nk_0a)\right)$$

so that (9) becomes

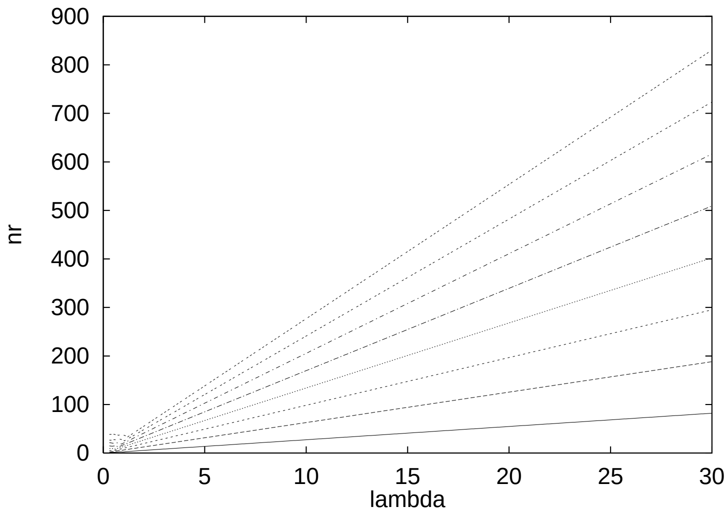

Figure 15: Grating resonances : Real part of the 8 root nearest to the origin in $\mathbf{H}_{||}$ polarization. ($\lambda/d \in [0.3, 30]$, $a = 0.14d$, evaluation for 400 wavelengths in the considered interval)

$$nJ_0(nk_0a)\left(-2 + (k_0a)^2\ln k_0d + i\frac{\pi k_0a^2}{d}\right) + 2J_1(nk_0a)\left(k_0a\ln\frac{d}{a} + i\frac{\pi a}{d}\right) \approx 0\ . \tag{15}$$

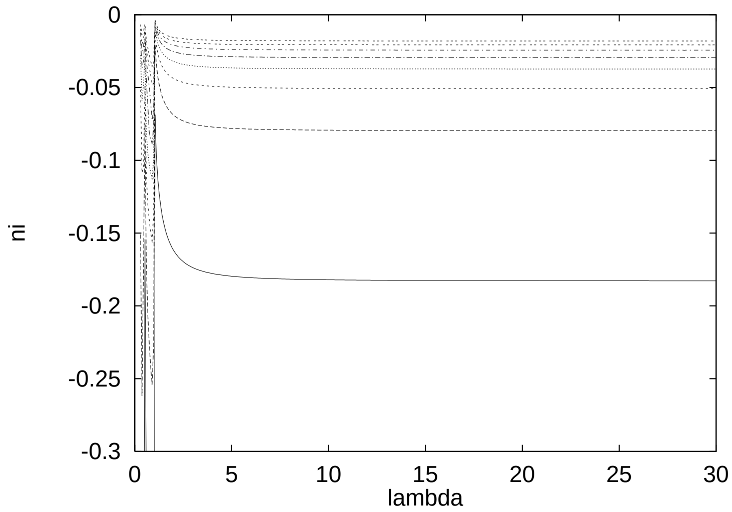

Figure 16: Grating resonances : Imaginary part of the same roots than in figure 16

All factors multiplying $J_1(nk_0a)$ and $nJ_0(nk_0a)$ tend to zero when k_0 approaches zero except the constant factors 2 and $i\pi a/d$, so that (15) can be simplified to

$$\frac{nk_0aJ_0(nk_0a)}{J_1(mk_0a)} \approx i\frac{\pi k_0a^2}{d} \tag{16}$$

for large λ. The right hand term of 16 tends to zero when k_0 approaches zero. If we assume that nk_0a remains bounded and non infinitesimal[11], the left hand term can can only be satisfied if $J_0(nk_0a)$ tends to zero. A first approximation to the roots is therefore the roots of $J_0(nk_0a) = 0$ which can be approximated by:

$$nk_0a \approx \pm\frac{(3+4m)\pi}{4},\ m \in \mathbb{N}$$

which gives us

$$n \approx \pm\frac{(3+4m)\lambda}{8a},\ m \in \mathbb{N}\ . \tag{17}$$

This again is a first order approximation for the resonant n, and gives us a good approximation of the real part of n. We will use the same method as

[11]If on the contrary nk_0a becomes infinitesimal, the same approximations as in 2.6.2 result in a non infinitesimal value of nk_0a, which is self-contradictory.

in 2.6.2 to find the imaginary part of the root: If $n^{(0)}$ is an approximation given by (17) we have

$$J_0(nk_0a) \approx J_0(n^{(0)}k_0a) + J_0'(n^{(0)}k_0a)in_ik_0a = -in_ik_0aJ_1(n^{(0)}k_0a)$$

so (16) gives us

$$n_i \approx -\frac{\pi}{n^{(0)}k_0d}$$

The complete set of resonances is therefore given by

$$n_m(\lambda) \approx \mathrm{sign}(m)\left(\frac{(3+4|m|)\lambda}{8a} - i\frac{4a}{(3+4|m|)d}\right),\ m \in \mathbb{Z} \qquad (18)$$

3 Off-axis incidence

In the general case, S_1 no longer equals zero, and equation (6) can not be simplified. Nevertheless we were able to modify our code without major complications to solve this new problem, as (6) can be changed in an equivalent analytic equation by the same means as in 2.5.

We computed the roots for various radii in the two polarizations, tracking them along λ and θ_0. We obtained about 20 Megabytes of data after a few days of intensive programming and computing, during which we also made advances in the analytic analysis of the behaviour of the roots. Unfortunately, when we analysed the data, it became obvious that there was an error in the code: we found resonating configurations with positive n_r and n_i, *ie* with a grating which should be damping. We found out there was a sign error in the lattice sum matrix, which we also used in our analytic work, cancelling all our work on off-axis incidence. The code has been corrected, and the computations started again, but the new results have not yet been fully analysed, nor has the analytic work led to significant results.

Nevertheless a few results emerge from the very first analysis:

- The roots with $n_i = 0$ corresponding to the antisymmetric dipole resonance become complex with $\theta_0 \neq 0$. This result is significant, as the symmetry argument (*cf.* 2.4) can not exclude these roots anymore.

- We have to be careful about the accuracy of our code. The accuracy seemed not to be very good for $\lambda < d$, as the results we obtained with the new program with $\theta_0 = 0$ differed significantly from the one we obtained with the code written for the normal incidence in that range. The cause of the error was not the new version of the program, nor the lack of accuracy of the lattice sums or the CROOT algorithm (which are both very accurate), but the fact that we computed fewer points for a given θ_0: For the normal incidence we usually computed 400 points of different λ, so the distance between a root for a given wavelength and the same root for the next wavelength was small. In the off-axis case we computed the roots for 80 wavelength for each θ_0, which was not enough to be sure to track the same root in the $\lambda < d$ region, where crossing of different roots are frequent : for $\lambda < d$ we obtained points almost randomly picked up among all the root-curves computed with 400 points[12].

For $\lambda > d$ the accuracy remains very good, as the coordinates of the roots do not change much with λ and θ_0, and the trajectories of the roots do not cross.

- Although we have checked carefully all the equations and the code, our set of data contains resonances with optical indices corresponding to non amplifying materials. These appear for some roots for $|\theta_0| > 1.2$ with large radii ($a = 0.3d$), so an accuracy problem could be an explanation, but they also appear within a nearly triangular shaped $\lambda - \theta_0$ region (see fig. 17) for all radii. This behaviour needs to be investigated in detail[13].

4 Conclusions

The resonances of a grating in normal incidence have been computed and estimated analytically; their behaviour with varying wavelength and refractive index have been understood mathematically. The studies of the normal incidence did not yield the clues we expected for the interpretation of unexplained stacked-gratings band-gaps, but the extension to off-axis incidence looks very promising on that point. The resonances we find for non amplifying materials are probably wrong, but can be explained by a lack of accuracy of the lattice sums in a λ-θ_0 region which is very close to the curve giving the passing off configurations for orders ± 1 (see figure 4.16 in [16]). If this hypothesis is correct, the behaviour of the roots in that region could

[12] remember footnote 10

[13] This investigation will not be easy, as a small k_0 expansion will not be sufficient, the 'anomalous' roots being in a region of finite k_0.

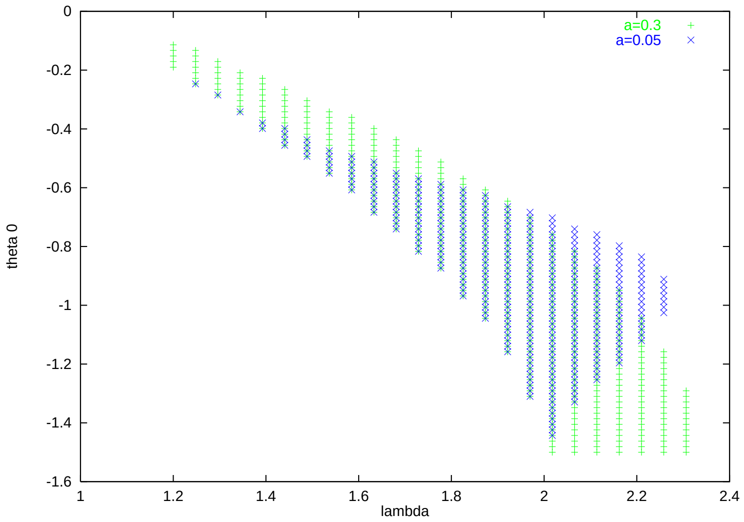

Figure 17: Resonances for non amplifying optical indices in $\mathbf{E}_{||}$ polarization, for $a = 0.3d$ and $a = 0.05d$

be very complex, and with an enhanced accuracy of the lattice sums some phenomena in stacked gratings might be understood through the resonances of a single grating.

During our work the question was raised whether the resonances of a grating could lead to a new way of homogenization: this would have been the case if for long wavelength nk_0a had become infinitesimal for all the roots. Through our analytic work, we have on the contrary proven that gratings can not be homogenized as far as the resonances are concerned: there can not be a layer of homogeneous refractive index and constant thickness which would have the same resonance behaviour as a grating, even for large wavelengths.

To obtain more information about surface states, the same study of the resonances should be undertaken with complex $\mathbf{k}_0$ (or alternatively with complex θ_0): this would give us an insight into the coupling of resonances with evanescent waves and therefore a better understanding of what happens at the surface of photonic crystals.

Personal conclusion

Although my contribution is very little by comparison with the work which has still to be done on the subject, I enjoyed a lot working on this current research topic, and it has encouraged me in my choice of my further studies. Before this traineeship I thought I could only enjoy experimental physics, but as I discovered the joys of theoretical physics (which after all are not so different from the pleasures of experimental physics) I understood that theory and experience are the two equally beautiful sides of a Möbius strip.

I would like to thank all the team - Ara Asatryan, Nicolae Nicorovici, Martijn de Sterke, Peter Robinson and Lindsay Botten - for being so welcoming and helpful, David Dawes for having the patience to help me when my computer refused to run and for (almost) saving my life when my hard drive refused to answer, and Samantha Mackinlay who fixed up all the administrative issues (even if I still don't have the Visa I would have needed).

I would particularly like to thank Dr. Ross McPhedran who accepted to supervise this traineeship, who always took the time to fill the gaps of my knowledge and to come and see the advances of my work, and who also introduced me to the rest of the team in which I felt treated as an equal.

I also would like to thank all Australians, from the unknown secretary in an unknown building who offered a coffee seeing the rings under my eyes on the first day after the flight, to the unknown retired people who gave my friends and me a big just-caught fish on a lonely beach, from the old lady who insisted on taking me to the bus stop when I didn't even ask her the way (but obviously looked completely lost) to the incredible farmer who welcomed my friends and me for two nights, gave us T-bone steaks and vegetables and taught us how to milk a cow, all of them having contributed to make my stay in Australia a wonderful time to remember. Thanks a lot.

Appendices

A Boundary Conditions

At the surface of the cylinders, the boundary conditions express the continuity of the tangential components of the fields. Thus depending on the polarization we obtain, the indices i and e meaning *interior* and *exterior*:

$$E_z^{(i)}\Big|_{r=a} = E_z^{(e)}\Big|_{r=a}\ ,\ \frac{1}{\mu_i}\frac{\partial E_z^{(i)}}{\partial r}\Bigg|_{r=a} = \frac{1}{\mu_e}\frac{\partial E_z^{(e)}}{\partial r}\Bigg|_{r=a} \tag{19}$$

for $\mathbf{E}_{||}$ polarization, and

$$H_z^{(i)}\Big|_{r=a} = H_z^{(e)}\Big|_{r=a}\ ,\ \frac{1}{\varepsilon_i}\frac{\partial H_z^{(i)}}{\partial r}\Bigg|_{r=a} = \frac{1}{\varepsilon_e}\frac{\partial H_z^{(e)}}{\partial r}\Bigg|_{r=a} \tag{20}$$

for $\mathbf{H}_{||}$ polarization.

Let $z = \varepsilon_e/\varepsilon_i$ for $\mathbf{H}_{||}$ polarization and $z = \mu_e/\mu_i$ for $\mathbf{E}_{||}$ polarization. We write V as a multipole expansion outside the cylinders

$$V^{(e)}(r,\theta) = \sum_{m\in\mathbb{Z}} \left[A_m J_m(k_0 r) + B_m Y_m(k_0 r)\right] e^{im\theta} \text{ for } r \geq a \tag{21}$$

and inside the cylinders, introducing a new set of coefficients C_m:

$$V^{(i)}(r,\theta) = \sum_{m\in\mathbb{Z}} C_m J_m(k^i r) e^{im\theta} \tag{22}$$

where $k^i = nk_0$ is the wave number inside the cylinders. Using the boundary conditions with these expansions yields, considering that the equations are true for all θ,

$$\left\{ \begin{array}{l} C_m J_m(nk_0 a) = A_m J_m(k_0 a) + B_m Y_m(k_0 a) \\ znC_m J'_m(nk_0 a) = A_m J'_m(k_0 a) + B_m Y'(k_0 a) \end{array} \right. \tag{23}$$

We can easily eliminate C_m of (23) and we then obtain a linear relation between A_m and B_m:

$$M_m = -\frac{A_m}{B_m} = \frac{znJ'_m(nk_0 a)Y(K_0 a) - Y'_m(k_0 a)J(nk_0 a)}{znJ'_m(nk_0 a)J(k_0 a) - J'_m(k_0 a)J_m(nk_0 a)} \tag{24}$$

As $z = 1/n^2$ for $\mathbf{H}_{||}$ polarization and $z = 1$ for $\mathbf{E}_{||}$ polarization, the result given in equation (4) should now be obvious.

B Lattice sums

The lattice sums

$$S_\ell = \sum_{p=1}^{\infty} H_\ell^{(1)}(pk_0 d)\left[e^{ipdk_0 \sin\theta_0} + (-1)^\ell e^{-ipdk_0 \sin\theta_0}\right] \tag{25}$$

are in general to slowly convergent in that form for numerical computation. Twersky [11] and McPhedran and Nicorovici [12] have developed methods to accelerate the convergence of the lattice sums. One method is to equate the spatial domain form [10, 12] and the spectral domain form of the Green's function associated with our problem:

$$Y_0(k_0 x) + S_0 J_0(k_0 x) + 2\sum_{\ell=1}^{\infty} S_\ell J_\ell(k_0 x) = \frac{2}{d}\sum_{m=-\infty}^{\infty} \frac{e^{i\alpha_m x}}{\chi_m}\,. \tag{26}$$

Here,

$$\alpha_m = k_0 \sin\theta_0 + mK, \quad K = \tfrac{2\pi}{d}, \quad m \in \mathbb{Z},$$

$$\chi_m = \begin{cases} \sqrt{k_0^2 - \alpha_m^2} & , \quad m \in \Omega = \{m|\alpha_m^2 < k_0^2\} \\ i\sqrt{\alpha_m^2 - k_0^2} & , \quad m \in \bar{\Omega} = \{m|\alpha_m^2 > k_0^2\}\,. \end{cases}$$

We split the lattice sums into two parts, according to the definition of Hankel functions $H_\ell^{(1)}(z) = J_\ell(z) + iY_\ell(z)$, to obtain

$$S_{2\ell} = S_{2\ell}^J + iS_{2\ell}^Y\,,$$

$$S_{2\ell+1} = iS_{2\ell+1}^J - S_{2\ell+1}^Y\,.$$

The lattice sums S_ℓ^J and S_ℓ^Y are oscillatory series and we have to use a summation method to evaluate them. Thus, for S_ℓ^J, by substituting in (26) we obtain the closed forms [10, 12]

$$S_{2\ell}^J = \frac{2}{d}\sum_{m\in\Omega} \frac{\cos\left[2\ell \sin^{-1}(\alpha_m/k_0)\right]}{\chi_m}\,,$$

$$S_{2\ell+1}^J = \frac{2}{d}\sum_{m\in\Omega} \frac{\sin\left[(2\ell+1) \sin^{-1}(\alpha_m/k_0)\right]}{\chi_m}\,.$$

For S_ℓ^Y we obtain representations in terms of absolutly convergent series over the reciprocal array. Thus, for $\ell = 0$ we have [11, 12]:

$$
\begin{aligned}
S_0^Y &= -\frac{2}{\pi}\left[\ln\frac{k_0}{2K}+\gamma\right]+\frac{1}{\pi}\left(\sum_{m=1}^{m_1}+\sum_{m=1}^{m_2}\right)\frac{1}{m} \\
&\quad -\frac{2}{d}\left\{\sum_{m=m_1+1}^{\infty}\left[\frac{1}{|\chi_m|}-\frac{1}{mK}\right]+\sum_{m=m_2+1}^{\infty}\left[\frac{1}{|\chi_{-m}|}-\frac{1}{mK}\right]\right\} ,
\end{aligned}
\tag{27}
$$

where m_1 and m_2 are defined by $\Omega = [-m_2, m_1]$, and γ is the Euler-Mascheroni constant. Analytic expressions for S_ℓ^Y have been given by Twersky [11], and in our notations they are:

$$
\begin{aligned}
S_{2\ell}^Y &= \frac{1}{\ell\pi}+\frac{1}{\pi}\sum_{m=1}^{\ell}\frac{(-1)^m 2^{2m}(\ell+m-1)!}{(2m)!(\ell-m)!}\left(\frac{K}{k_0}\right)^{2m}B_{2m}(\alpha_0/K) \\
&- \frac{2}{d}\left(\sum_{m=0}^{m_1}-\sum_{m=-1}^{-m_2}\right)\frac{\sin[2\ell\sin^{-1}(\alpha_m/k_0)]}{\chi_m} \\
&- (-1)^\ell\frac{2}{d}\left\{\sum_{m=m_1+1}^{\infty}\frac{[(\alpha_m-|\chi_m|/k_0]^{2\ell}}{|\chi_m|}+\sum_{m=m_2+1}^{\infty}\frac{[(-\alpha_{-m}-|\chi_{-m}|/k_0]^{2\ell}}{|\chi_{-m}|}\right\} ,
\end{aligned}
\tag{28}
$$

$$
\begin{aligned}
S_{2\ell+1}^Y &= \frac{2}{\pi}\sum_{m=0}^{\ell}\frac{(-1)^m 2^{2m}(\ell+m)!}{(2m+1)!(\ell-m)!}\left(\frac{K}{k_0}\right)^{2m+1}B_{2m+1}(\alpha_0/K) \\
&- \frac{2}{d}\left(\sum_{m=0}^{m_1}-\sum_{m=-1}^{-m_2}\right)\frac{\cos[(2\ell+1)\sin^{-1}(\alpha_m/k_0)]}{\chi_m} \\
&- (-1)^\ell\frac{2}{d}\left\{\sum_{m=m_1+1}^{\infty}\frac{[(\alpha_m-|\chi_m|/k_0]^{2\ell+1}}{|\chi_m|}+\sum_{m=m_2+1}^{\infty}\frac{[(-\alpha_{-m}-|\chi_{-m}|/k_0]^{2\ell+1}}{|\chi_{-m}|}\right\} ,
\end{aligned}
\tag{29}
$$

where B_m are Bernoulli polynomials. Note that, in (28) and (29) we have $\alpha_{-m} < 0$.

References

[1] J. Dowling, H. Everitt, and E. Yablonovitch. Photonic and acoustic band-gap biliography. http://home.earthlink.net/ jpdowling/pbgib.html.

[2] J. D. Joannopoulos, R. D. Medde, and J. N. Winn. *Photonic Crystals, Molding the flow of light*. Princeton University Press, 1995.

[3] Joannopolous Research Group. Photonic crystal research web page. http://ab-initio.mit.edu/photons/index.html.

[4] L. C. Botten, N. A. Nicorovici, R. C. McPhedran, A. A. Asatryan, C. M. de Sterke, and P. A. Robinson. Electromagnetic diffraction by stacked gratings of metallic and dielectric cylinders: Formulation and analytic properties. To be published.

[5] R. C. McPhedran and D. R. McKenzie. Electrostatic and optical resonances of arrays of cylinders. *Appl. Phys.*, 23:223–235, 1980.

[6] R. C. McPhedran and W. T. Perrins. Electrostatic and optical resonances of cylinder pairs. *Appl. Phys.*, 24:311–318, 1981.

[7] D. J. Bergman. The dielectric constant of a composite material - a problem in classical physics. *Phys.Rep.*, 43(9):377–407, 1978.

[8] Lord Rayleigh. On the influence of obstacles arranged in rectangular order upon the properties of a medium. *Philos. Mag.*, 34:481–502, 1892.

[9] W. v. Ignatowsky. Zur Theorie der Gitter. *Ann. Physik*, 44:369–436, 1914.

[10] R. C. McPhedran, N. A. Nicorovici, L. C. Botten, and Bao Ke-Da. Green's function, lattice sums and Rayleigh's identity for a dynamic scattering problem. In G. Papanicolau, editor, *IMA Volumes in Mathematics and its Applications*, volume 96, pages 155–186. Springer Verlag, New York, 1997.

[11] V. Twersky. Elementary function representations of Schlömlich series. *Arch. Rational Mech. Anal.*, 8:323–332, 1961.

[12] N. A. Nicorovici and R. C. McPhedran. Lattice sums for off-axis electromagnetic scattering by gratings. *Phys. Rev. E*, 50:3143–3160, 1994.

[13] W. T. Perrins, D. R. McKenzie, and R. C. McPhedran. Transport properties of regular arrays of cylinders. *Proc. R. Soc. Lond. A*, 369:207–225, 1979.

[14] L. C. Botten, M. S. Craig, and R. C. McPhedran. Complex zeros of analytic functions. *Computer Physics Communications*, 29:245–259, 1983.

[15] R. W. Wood. *Proc. Phys. Soc.*, 18:396, 1902.

[16] M. C. Hutley. *Difraction Gratings.* Academic Press, 1982.

Abstract

With the aim of explaining anomalous peaks in the optical absorption spectrum of stacked gratings of cylinders, which are photonic bang gap material, we study the resonances of a single grating theoretically. We derive the main equation of the resonances using the Generalized Rayleigh Method and truncate it to the second order of multipole expansion. We investigate extensively the behaviour of the roots of this equation numerically and analytically in the case of normal incidence. The work on the more general case of off-axis incidence is not finished yet but preliminary results are given. Achieving the analysis of the off-axis case is essential if we want to obtain insights in the behaviour of stacked gratings.